ChemComm

COMMUNICATION

View Article Online
View Journal | View Issue

Cite this: *Chem. Commun.*, 2014, **50**, 15212

Received 13th July 2014,
Accepted 9th October 2014

DOI: 10.1039/c4cc05390g

www.rsc.org/chemcomm

Microtubes and hollow microspheres formed by winding of nanoribbons from self-assembly of tetraphenylethylene amide macrocycles†

Song Song,[a] Hua-Fei Zheng,[b] Hai-Tao Feng[a] and Yan-Song Zheng*[a]

New amide macrocycles based on tetraphenylethylene (TPE) were synthesized. It was found that the TPE amide macrocycles could form microtubes in H_2O–THF with 70–80% water by the rolling up of big nanoribbons but produced hollow microspheres in 90% or more water by the winding of thin nanoribbons. The microtubes emitted blue light while the hollow microspheres showed blue-green fluorescence.

Macrocyclic compounds such as crown ethers, cyclodextrins and calixarenes not only are well-known for their excellent properties in molecular recognition but are also very outstanding in self-assembling micro/nanomaterials by the macrocyclic skeleton,[1] therefore, they are always attracting extensive attention. With new structures and new functional groups, new macrocycles give us bigger research space, but the availability of new macrocycles with both novel structures and excellent properties is still very limited.[2,3] Recently it has been found that tetraphenylethylene (TPE) and its derivatives have a novel aggregation-induced emission (AIE) effect due to the unique propeller structure of the TPE unit, and exhibit great potential for bio/chemosensors and solid emitters.[4] Connecting the TPE unit(s) into macrocycles by different linkages is likely to give a new class of excellent macrocycles due to the unique propeller-like structure, novel AIE effect, and easy modification of the four phenyl rings of the TPE unit.[5] In fact, some Schiff base macrocycles based on TPE have exhibited high selectivity and sensitivity in the detection of explosive dinitrophenol and copper ions.[5a,b] Herein, we report that new amide macrocycles based on TPE can self-assemble into nanoribbons in aqueous media. Unexpectedly, the nanoribbons can roll into microtubes and enwind into hollow microspheres in a mixed solvent of water and THF with different water fractions.

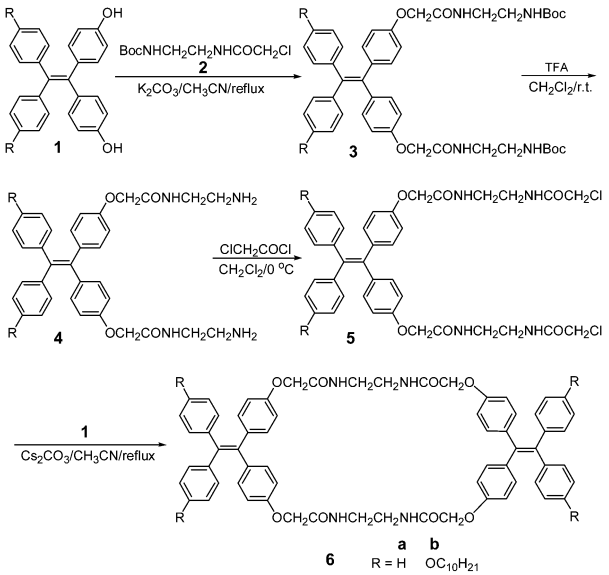

Scheme 1 Synthesis route of the TPE amide macrocycles **6**.

The TPE amide macrocycles **6a** and **6b** were synthesized according to the synthetic route shown in Scheme 1. Nucleophilic substitution of *N*-Boc-*N*′-chloroacetylethylenediamine **2**[6] by dihydroxyl TPE **1** (a known AIE compound)[7] in the presence of potassium carbonate offered **3**, which was transferred into TPE diamine **4** by removal of the Boc protecting groups in trifluoroacetic acid (TFA)–dichloromethane solvent. After treatment with chloroacetyl chloride in the presence of triethylamine, the dichloride **5** was obtained. After one more nucleophilic substitution with dihydroxyl TPE **1** in the presence of cesium carbonate, the dichloride **5** was converted into the TPE amide macrocycle **6** in about 33% yield. The macrocycles were fully characterized by ^{1}H NMR, ^{13}C NMR, FT-IR, and HRMS spectra.

Macrocycle **6a** had very little solubility in conventional solvents but was soluble in DMF. The solution of **6a** in DMF

[a] *Key Laboratory for Large-Format Battery Materials and System, Ministry of Education, School of Chemistry and Chemical Engineering, Huazhong University of Science and Technology, Wuhan 430074, China. E-mail: zyansong@hotmail.com; Fax: +86-27-87543632; Tel: +86-27-87543232*

[b] *School of Chemistry and Materials Science, University of Science and Technology of China, Hefei 230026, China*

† Electronic supplementary information (ESI) available: Experimental materials and methods, spectra and crystal structure. CCDC 1013554. For ESI and crystallographic data in CIF or other electronic format see DOI: 10.1039/c4cc05390g

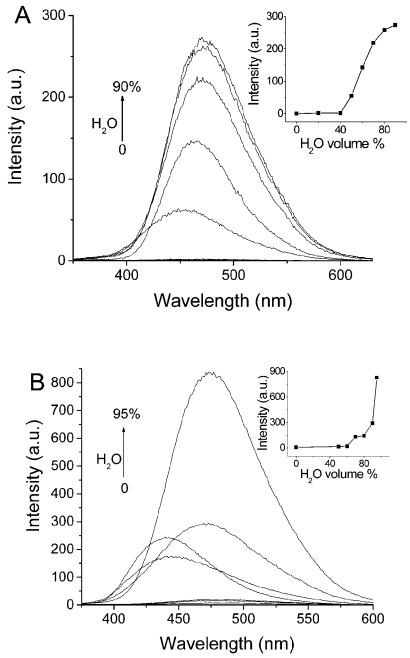

Fig. 1 Change in the fluorescence spectra of **6a** (A) and **6b** (B) in a mixed solvent of H_2O–DMF (A) or H_2O–THF (B) with water fraction. Inset, curve of fluorescence intensity *versus* water fraction at 470 nm (A) and at 475 nm (B). [**6a**] = 5×10^{-5} M, [**6b**] = 2×10^{-5} M, λ_{ex} = 323 nm, ex/em slits = 3/3 nm.

did not emit light while the solid **6a** emitted strong blue fluorescence. By the addition of up to 40% (volume ratio, the same below) non-solvent water into the solution of **6a** in DMF, the solution became turbid and the resultant suspension started to emit light. After that, the fluorescence of **6a** increased as the water fraction increased (Fig. 1A). These results indicated that macrocycle **6a** was an AIE compound. Meanwhile, the emission maximum wavelength λ_{max} showed a bathochromic shift from 450 nm to 470 nm. Similarly, the solution of **6b** in a common organic solvent which could dissolve it emitted no light while its solid showed strong blue fluorescence. With the increase of water fraction, the suspension of **6b** in H_2O–THF also exhibited increasing fluorescence intensity and an even bigger bathochromic shift of emission λ_{max} from 440 nm to 475 nm (Fig. 1B). Under irradiation of a UV lamp at 365 nm, an obvious color change from blue to blue-green could be seen by the naked eye when the water fraction was raised from 80% to more than 90% (Fig. 2). The dry solid obtained by centrifugation separation of the suspension of **6b** displayed a similar colour change as the suspension under UV light, which

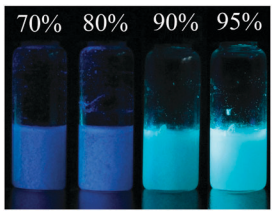

Fig. 2 Photograph of a suspension of **6b** (1.0×10^{-3} M) in H_2O–THF with increasing water fraction under irradiation of a UV lamp at 365 nm.

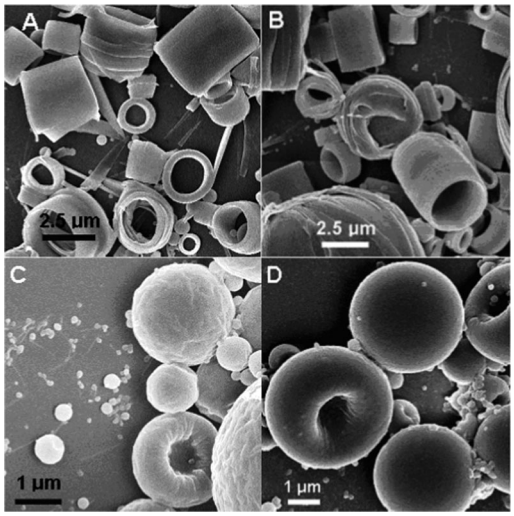

Fig. 3 FE-SEM images of the suspension of **6b** in H_2O–THF with water fractions of 70% (A), 80% (B), 90% (C) and 95% (D). [**6b**] = 1.0×10^{-3} M.

excluded the effect of the solvent polarity on the emission (Fig. S14 and S15, ESI†).

The emission λ_{max} change or the color change of the suspension with water fraction is sometimes due to different morphologies of the aggregates in a suspension, therefore, the suspension of **6b** in H_2O–THF was examined by electron microscopy. Interestingly, the morphology of the aggregates of **6b** in the mixed solvent truly changed with the increase in water fraction. It was disclosed by FE-SEM images that the suspension in 70 : 30–80 : 20 H_2O/THF was mainly composed of microtubes in addition to minor nanoribbons (Fig. 3A and B). The microtubes had a diameter of 0.3–3.0 μm and a wall thickness of 0.1–0.5 μm, but their length was only 0.3 μm to 4 μm, which was short compared with their large diameter and made them appear like short hollow cylinders. Unexpectedly, the microtubes were formed by the self rolling of nanoribbons which had a width of 100–500 nm and length of several micrometers, because the nanoribbons that wrapped on the surface of the microtubes could be seen clearly. Moreover, a final section of a nanoribbon that could not finish the rolling up could also be seen from the outside of a microtube. TEM images confirmed the formation of the microtubes by the rolling of the nanoribbons because a length of nanoribbon was clearly pulled out from the surface of a microtube and a layer-like structure of the wall of the microtube was observed (Fig. 4A and B and Fig. S16 and S17, ESI†).

When the water fraction was increased to 90%, the suspension was made of microspheres with a diameter of 1–5 μm and minor nanoribbons with a diameter of about 80 nm. On the surface of some microspheres, a sunken hole could be seen, indicating that the microspheres were probably hollow. Meanwhile, there were many thin nanoribbons like wrinkles on the surface of the microsphere, which had almost the same diameter as the discrete nanoribbons. Therefore, the microspheres were formed by the wrapping of the nanoribbons, just like winding wool into a ball. TEM images corroborated that the microspheres came from the winding of thinner nanoribbons and were hollow (Fig. 4C, D and Fig. S18, S19, ESI†). Meanwhile, a few nanoribbons which were

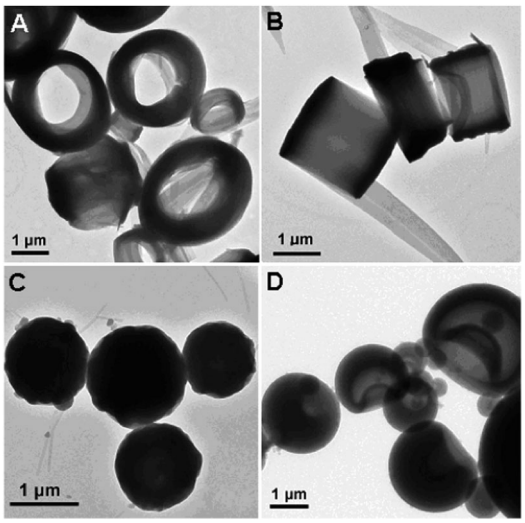

Fig. 4 TEM images of the suspension of **6b** in H_2O–THF with water fractions of 70% (A), 80% (B), 90% (C) and 95% (D). [**6b**] = 1.0×10^{-3} M.

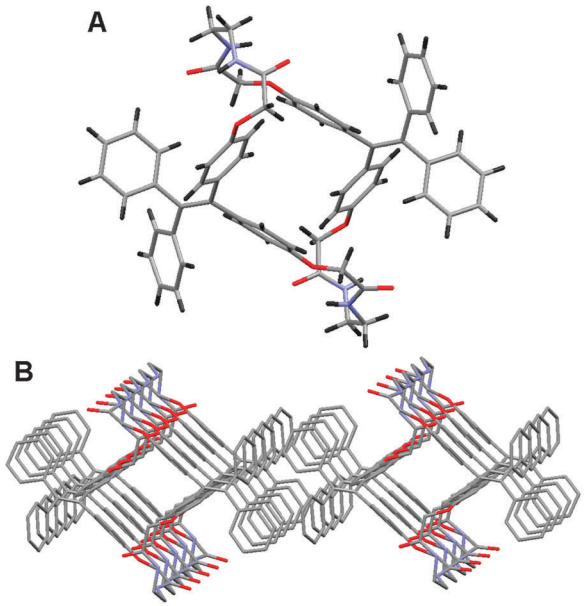

Fig. 5 Crystal structures of **6a** (A) and the formation of 2D nanoribbons by intermolecular stacking in the crystal state (B). The solvent molecules and hydrogen atoms in B are omitted for clarity.

about 1 μm long and 80 nm wide were found, further demonstrating that the nanoribbons that formed in solvents with a higher water fraction were thinner than those in low water fractions, which was in accordance with the FE-SEM observation. When the water fraction was raised to 95%, both FE-SEM and TEM images disclosed that the suspension was composed of hollow microspheres with a diameter of 1–5 μm, but no nanoribbons were found in the images. The surface of the microspheres was smoother than that of the microspheres in 90 : 10 H_2O/THF, as they were probably wound from thinner nanoribbons. Unlike **6b**, the suspension of **6a** in 95 : 5 H_2O/DMF only gave nanoribbons instead of microspheres (Fig. S20, ESI†) and did not exhibit the colour change with increasing water fraction under UV light.

Single crystals of **6a** suitable for X-ray diffraction analysis were obtained in DMF–water mixed solvent.[8] Like all of the crystal structures of TPE derivatives, the TPE unit of **6a** had a propeller-like structure in order to reduce the repulsion between neighboring aromatic rings. The ethylenediamide linkage between the two TPEs formed a twisted structure due to intramolecular hydrogen bonds, which resulted in a cavity of **6a** which was smaller than expected (Fig. 5A). But molecules of **6a** could still stack each other from cavity to cavity to form a 1D network through ArH–O hydrogen bonds and ArH–π interactions (Fig. 5B and Fig. S21, ESI†). Between two 1D networks, there were ArH–π interactions which could lead to the production of a 2D network, that is, nanoribbons. For **6b**, in addition to the ArH–π interactions from cavity to cavity, the long alkyl chains have strong van de Waals attractions and hydrophobic forces, which would expedite the formation of the nanoribbons.

In the mixed solvent of H_2O–THF with a lower water fraction, the aggregation velocity of **6b** was not large, so that the macrocycle could grow into big nanoribbons. Meanwhile, **6b** was in a more stable conformation in which the aromatic rings had less conjugation with double bonds and less repulsive forces between them. Therefore, the suspension of **6b** in the mixed solvent with a low water fraction emitted a shorter wavelength of light. In contrast, when the water fraction was raised to 90–95%, the aggregation of **6b** was so fast that it did not have time to grow into big nanoribbons but only resulted in thinner nanoribbons. The thinner nanoribbons were easily wound up into spheres. Due to a high content of water, the larger hydrophobic force compelled the macrocycle existence to a less stable conformation in which the aromatic rings had more conjugation with double bonds but larger repulsive forces between them. Therefore, the suspension of **6b** in 90–95% water showed an emission with an obvious bathochromic shift. By rolling the big nanoribbons into microtubes or winding the thin ones into hollow microspheres, the hydrophobic forces of molecules of **6b** could be attenuated. After grinding, the emission of a powder of **6a** or **6b** changed from blue light to blue-green light, and after exposure to organic solvent, the blue-green powder went back into a blue one quickly (Fig. S22 and S23, ESI†).[9] This result also indicated that external force, just like the hydrophobic force, could enforce the amide macrocyclic molecules to be in a conformation with higher energy, in which the aromatic rings had more conjugation with double bonds and more repulsion between them.

By slow precipitation of **6b** from the mixed solvent of CH_2Cl_2 and CH_3OH, the obtained solid exhibited many sharp and strong peaks in the powder X-ray diffraction (XRD) pattern, indicating that it was crystalline (Fig. 6A). The powder obtained by centrifugation of a suspension of **6b** in 70% water had some sharp peaks in the XRD pattern but both the number and the intensity were less, demonstrating less crystal structure (Fig. 6B). This is in accordance with the self-rolling of the nanoribbons into microtubes which were more isotropic than the nanoribbons. The powder from 95% water was composed of hollow microspheres which were totally isotropic due to the random winding of thin nanoribbons around a round space. Therefore, it was amorphous and had no sharp peaks in the XRD pattern (Fig. 6C).

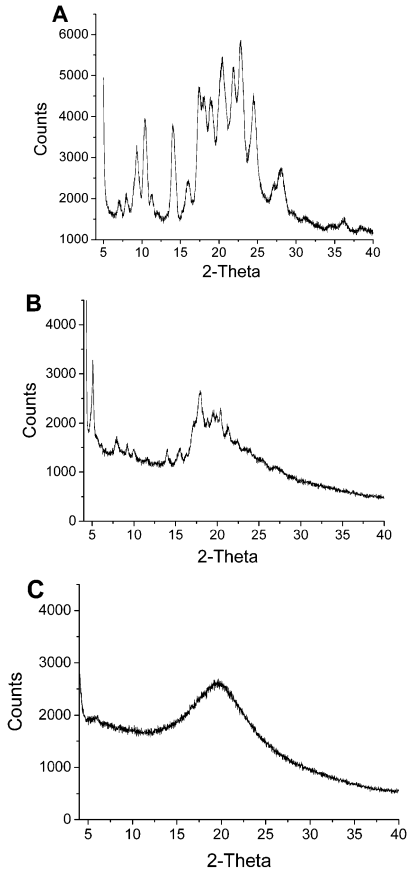

Fig. 6 Powder X-ray diffraction pattern of the dry solid of **6b** resulting from recrystallization by CH_2Cl_2–CH_3OH (A) and from the suspension in H_2O–THF with a water fraction of 70% (B) and 95% (C).

In conclusion, two novel TPE amide macrocycles with AIE effects were synthesized. It was found that the macrocycle could form microtubes and hollow microspheres in H_2O–THF with an increase of water fraction. In 70–80% water, the macrocyclic molecules could self-assemble into bigger nanoribbons which could roll up into microtubes. In 90% or more water, the macrocyclic molecules self-assembled into very thin nanoribbons which wound into hollow microspheres. The microtubes composed of big nanoribbons emitted blue light but the hollow microspheres showed blue-green fluorescence due to different conformations of the macrocycle. This interesting finding provided a new approach for the preparation of microtubes and hollow microspheres just by changing the water fraction.

The authors thank the National Natural Science Foundation of China (No. 21072067) and the Analytical and Testing Centre at Huazhong University of Science and Technology for support.

Notes and references

1 (*a*) K. Kim, N. Selvapalam, Y. H. Ko, K. M. Park, D. Kim and J. Kim, *Chem. Soc. Rev.*, 2007, **36**, 267–279; (*b*) J. Zhang, R. J. Coulston, S. T. Jones, J. Geng, O. A. Scherman and C. Abell, *Science*, 2012, **335**, 690–694; (*c*) V. Haridas, S. Sahu and A. R. Sapala, *Chem. Commun.*, 2012, **48**, 3821–3823; (*d*) H. Huang, D.-M. Li, W. Wang, Y.-C. Chen, K. Khan, S. Song and Y.-S. Zheng, *Org. Biomol. Chem.*, 2012, **10**, 729–735.

2 (*a*) W.-Y. Yang, J.-H. Ahn, Y.-S. Yoo, N.-K. Oh and M. Lee, *Nat. Mater.*, 2005, **4**, 399–402; (*b*) I. Alfonso, M. Bru, M. I. Burguete, E. García-Verdugo and S. V. Luis, *Chem. – Eur. J.*, 2010, **16**, 1246–1255; (*c*) Y. Kim, S. Shin, T. Kim, D. Lee, C. Seok and M. Lee, *Angew. Chem., Int. Ed.*, 2013, **52**, 6426–6429; (*d*) S. Lee, C.-H. Chen and A. H. Flood, *Nat. Chem.*, 2013, **5**, 704–710.

3 (*a*) M. C. O'Sullivan1, J. K. Sprafke1, D. V. Kondratuk, C. Rinfray, T. D. W. Claridge, A. Saywell, M. O. Blunt, J. N. O'Shea, P. H. Beton, M. Malfois and H. L. Anderson, *Nature*, 2011, **469**, 72–75; (*b*) J. T. A. Jones, T. Hasell, X. Wu, J. Bacsa, K. E. Jelfs, M. Schmidtmann, S. Y. Chong, D. J. Adams, A. Trewin, F. Schiffman, F. Cora, B. Slater, A. Steiner, G. M. Day and A. I. Cooper, *Nature*, 2011, **474**, 367–371.

4 (*a*) Y. Hong, J. W. Y. Lam and B. Z. Tang, *Chem. Soc. Rev.*, 2011, **40**, 5361–5388; (*b*) M. Wang, G. Zhang, D. Zhu and B. Z. Tang, *J. Mater. Chem.*, 2010, **20**, 1858–1867.

5 (*a*) H.-T. Feng and Y.-S. Zheng, *Chem. – Eur. J.*, 2014, **20**, 195–201; (*b*) H.-T. Feng, S. Song, Y.-C. Chen, C. H. Shen and Y.-S. Zheng, *J. Mater. Chem. C*, 2014, **2**, 2353–2359; (*c*) J.-H. Wang, H.-T. Feng, J. Luo and Y.-S. Zheng, *J. Org. Chem.*, 2014, **79**, 5746–5751; (*d*) S. Song and Y.-S. Zheng, *Org. Lett.*, 2013, **15**, 820–823; (*e*) C. Zhang, Z. Wang, S. Song, X. Meng, Y.-S. Zheng, X.-L. Yang and H.-B. Xu, *J. Org. Chem.*, 2014, **79**, 2729–2732.

6 A.-M. Fanning, S. E. Plush and T. Gunnlaugsson, *Chem. Commun.*, 2006, 3791–3793.

7 X.-F. Duan, J. Zeng, J.-W. Lü and Z.-B. Zhang, *J. Org. Chem.*, 2006, **71**, 9873–9876.

8 CCDC 1013554.

9 (*a*) X. Luo, W. Zhao, J. Shi, C. Li, Z. Liu, Z. Bo, Y. Q. Dong and B. Z. Tang, *J. Phys. Chem. C*, 2012, **116**, 21967–21972; (*b*) C. Li, X. Luo, W. Zhao, C. Li, Z. Liu, Z. Bo, Y. Dong, Y. Q. Dong and B. Z. Tang, *New J. Chem.*, 2013, **37**, 1696–1699.